



HAL
open science

Phase-matching-free ultrashort laser pulse characterization from transient plasma lens

R K Bhalavi, P. Béjot, A Leblanc, A Dubrouil, Franck Billard, Olivier
Faucher, Edouard Hertz

► **To cite this version:**

R K Bhalavi, P. Béjot, A Leblanc, A Dubrouil, Franck Billard, et al.. Phase-matching-free ultrashort laser pulse characterization from transient plasma lens. Optics Letters, In press. hal-04445900

HAL Id: hal-04445900

<https://hal.science/hal-04445900>

Submitted on 8 Feb 2024

HAL is a multi-disciplinary open access archive for the deposit and dissemination of scientific research documents, whether they are published or not. The documents may come from teaching and research institutions in France or abroad, or from public or private research centers.

L'archive ouverte pluridisciplinaire **HAL**, est destinée au dépôt et à la diffusion de documents scientifiques de niveau recherche, publiés ou non, émanant des établissements d'enseignement et de recherche français ou étrangers, des laboratoires publics ou privés.

Phase-matching-free ultrashort laser pulse characterization from transient plasma lens.

R. K. BHALAVI^{1,2}, P. BÉJOT¹, A. LEBLANC³, A. DUBROUIL², F. BILLARD¹, O. FAUCHER¹, AND E. HERTZ^{1,*}

¹Laboratoire Interdisciplinaire Carnot de Bourgogne, UMR CNRS 6303 - Université de Bourgogne, 21078 Dijon Cedex, France

²Femto Easy, Batiment Gienah, Cité de la Photonique, 11 avenue de Canteranne, 33600 Pessac France.

³Laboratoire d'Optique Appliquée, Ecole Polytechnique, ENSTA, CNRS, Université Paris Saclay, Palaiseau, France.

*Corresponding author: edouard.hertz@u-bourgogne.fr

Compiled January 31, 2024

A phase-matching free ultrashort pulse retrieval based on the defocusing of a laser-induced plasma is presented. In this technique, a pump pulse ionizes a rare gas providing a plasma lens whose creation time is ultrafast. A probe pulse propagating through this gas lens experiences a switch of its divergence. The spectrum of the diverging part, isolated by a coronagraph, is measured as a function of the pump-probe delay, providing a spectrogram that allows for a comprehensive characterization of the temporal properties of the probe pulse. The method, called PI-FROSt for “Plasma-Induced Frequency resolved Optical Switching”, is simple, free of phase matching constraints, and can operate in both self- and cross-referenced configurations at ultra-high repetition rate in the whole transparency range of the gas. The assessment of the method demonstrates laser pulse reconstructions of high reliability in both near-infrared and ultraviolet spectral ranges. © 2024 Optical Society of America

OCIS codes: (190.7110) Ultrafast nonlinear optics; (320.7080) Ultrafast devices; (320.0320) Ultrafast optics; (320.7100) Ultrafast measurements.

<http://dx.doi.org/10.1364/ao.XX.XXXXXX>

Since its inception, the field of laser technology has known major technological breakthroughs, one of the most spectacular being undoubtedly the generation of ultrashort laser pulses. The properties of such sources, with femtoseconds (fs) scale durations, have rapidly become invaluable opening up a realm of unprecedented prospects in various areas, ranging from cutting-edge scientific research to applications in industrial and medical fields. Over the last decades, the generation of ultrashort pulses has witnessed remarkable advancements with the emergence of new coherent sources in the infrared (IR) and ultraviolet (UV), the generation of super-continua [1], IR [2] or Terahertz [3] near-single cycle pulses, and XUV attosecond pulses [4]. To harness the full potential of fs laser pulses, a comprehensive characterization of the electric field is crucial. This led to a growing interest in reliable, versatile and innovative diagnostic tools [5] driven with the advancement of sources with increasingly shorter du-

rations or broader wavelength ranges. A wide array of optical methods enabling the characterization of ultrashort laser pulses have been thus developed in which Frequency-Resolved Optical Gating [5, 6] (FROG) and Spectral Phase Interferometry for Direct Electric-Field Reconstruction [5, 7] (SPIDER) have emerged as the two most widely used self-referenced complete characterization tools. Other approaches [8–10] have also triggered notable interests. The developed approaches mostly rely on a mechanism of frequency conversion through a nonlinear parametric process, a phenomenon which suffers from phase-matching constraints. They can therefore hardly be applied to the measurement of ultra-broadband pulses as super-continuum or a set of harmonic fields. The phase matching conditions can be relaxed by the use of third order non-linearities as implemented in transient grating FROG, polarization-gated FROG [6], or DEER-SPIDER [11], even though it should be emphasized that the latter two imply the use of polarizers, while the first one is not phase-matched in a two color configuration [12]. Recently, A. Leblanc *et al.* [13] reported a characterization technique called Frequency Resolved Optical Switching (FROSt) which overcomes the issue of phase matching constraints. FROSt relies on the temporal slicing of a test pulse induced by the sudden drop of a semiconductor’s transmission. A fs “pump” pulse, of central wavelength within the absorption band of a semiconductor is absorbed by the latter. The process promotes electrons to the conduction band leading to a sudden transmission drop. This switch of optical transmission can be seen as a “temporal knife-edge” for a probing pulse. The “probe” pulse, whose spectrum lies in the transmission band of the semiconductor, interacts with this temporal knife. Depending on the pump-probe relative delay, the switch transmits the portion of the probe pulse arriving before the pump and reflects the other part. The spectrum of the transmitted field is measured as a function of the delay providing a spectrogram (time-frequency map) that is processed using a ptychographic algorithm to retrieve both the probe and optical switch temporal profiles. FROSt technique provides a phase-matching-free signal. This exceptional property made possible the characterization of pulses over a broad range of wavelengths from 0.7 to 10 microns [13] and supercontinua with ultrabroad spectra spanning over more than 2 octaves [14]. In addition, the method can operate in both scanning [13]

and single-shot operations [15]. The FROSt technique features nevertheless some limitations. First, considering the spectral transmission bands of semiconductors, it can mainly characterize pulses spanning from mid-IR to visible range but does not operate in the UV due to the lack of transparent semiconductors (less user-friendly approaches [16, 17] requiring displacement of material between consecutive laser shots have been proposed in this issue). Second, the inherent FROSt arrangement relies on a cross-referenced measurement with a pump and probe of different wavelengths, lying in the absorption and transmission band of the semiconductor, respectively. Such a conventional two-color configuration restricts the method's suitability for self-referenced measurements, at least, in standard use (note that FROSt characterization with pump and probe of same color has been shown to be possible [15]). Lastly, the pump energy with standard FROSt configuration is quite substantial since a pump beam of large cross-section is necessary to ensure spatially homogeneous transmission switching for the probe beam. The aforementioned issues may constitute limiting factors for various applications. We propose, in this Letter, a new variant of the frequency resolved optical switching strategy that targets its intended purpose but features the ability to address the notoriously challenging characterization in the UV range and boasts additional strengths discussed below. The method called PI-FROSt for "Plasma Induced FROSt" relies on the cross-defocusing of a probe pulse through a plasma lens. In PI-FROSt, a plasma lens is induced via non-resonant multiphoton ionization process by focusing a moderately intense pump pulse in a rare gas. The creation time of the plasma lens is ultrafast so that it can act as a prompt temporal switch to diffract a part of a probe pulse (the portion arriving subsequent to the pump pulse). A probe pulse, focused at the same spot as the pump, thus experiences a switch of divergence. The increase of its beam size in the far field is isolated by a coronagraph and measured by a spectrometer as a function of the pump-probe delay. This provides a spectrogram enabling a complete characterization of the temporal and spectral characteristics of the probe. The method is simple, free of phase matching constraints, can operate in both self- and cross-referenced configurations, and features other remarkable assets that could prove highly valuable to the scientific community of ultrafast laser fields. The potentiality of PI-FROSt is assessed here through the characterization of fs pulses in the near-infrared (NIR) and UV spectral domain ($\lambda = 802$ nm and 266 nm, respectively) using a pump pulse centered at $\lambda = 802$ nm.

The experimental set-up is described in Fig. 1. A Ti:Sapphire

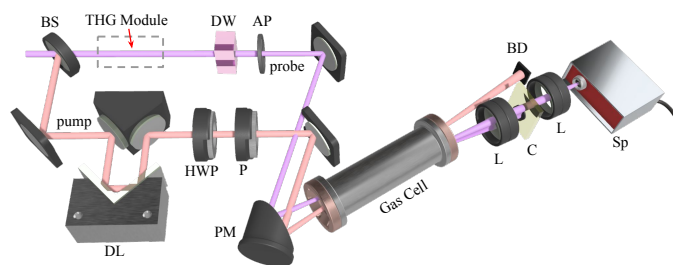


Fig. 1. Experimental set-up. BS, beam splitter; DL, delay line; HWP, half-waveplate; P, polarizer; PM, parabolic mirror; DW, dispersive window; AP, aperture; BD, beam dump; C, coronagraph; L, lens; Sp, spectrometer [FLAME (resp. USB4000) from Ocean Optics for IR (resp. UV)].

laser source delivers laser pulses of 35 fs FWHM duration centered at $\lambda = 802$ nm at 1 kHz repetition rate. A beam splitter (BS) divides the laser beam into two arms to provide the pump and probe beams. The probe pulse, to be characterized, is centered either at the pump wavelength or at its third harmonic. In the last case, a third-harmonic generation (THG) module (providing a sum frequency mixing between fundamental and second harmonic fields) is inserted into the path of the probe. In order to test the reliability of the pulse reconstruction, various calibrated dispersive windows (DW) made of SF₁₁ [resp. Fused Silica (FS)] for NIR [resp. UV] measurements can be used so as to induce specific chirp. The pump pulse is time-delayed with a motorized delay line (DL). Its energy and polarization can be controlled by a half-waveplate (HWP) and a polarizer (P). Pump and probe polarizations are crossed so as to minimize a potential contribution from the electronic Kerr effect, which is found to be negligible under these conditions. The two beams are then focused with a slight angle ($\approx 3^\circ$) into a gas cell with an off-axis parabolic mirror ($f=20$ cm) on which the two arrive collinearly. The cell, of 1 mm thick FS entrance window, is filled with 1 bar of Ar. At the exit of the cell, after being collimated by a lens (L), the probe beam is blocked out by a coronagraph (C). The size of the coronagraph is adjusted so as to perfectly match the probe beam's profile and completely block it in the absence of ionization (i.e. with the pump off). In the presence of plasma, the beam size increases in the far field. The unblocked portion of the probe beam propagating behind the coronagraph is measured by a spectrometer as a function of the pump-probe delay τ to provide a spectrogram $S(\omega, \tau)$. This last enables the reconstruction of the probe pulse temporal profile. The plasma is generated via non-resonant multi-photon ionization process that is governed by the ionization probability: $P(I_{pu}) \propto I_{pu}^{NL}$, where I_{pu} is the pump intensity and NL the effective non-linearity factor. If one considers a standard Gaussian spatial distribution for I_{pu} at the focal point, the electron density n_e decreases with the radial coordinate r . The plasma therefore behaves like a diverging lens since the refractive index variation depends negatively on the electron density as $\Delta n = -n_e / (2n_{cr})$, where n_{cr} is the critical density. In the time domain, as the pump pulse enters into the focusing region, the density of free electrons gradually increases and accumulates so as to form a time-dependent electron density. The refractive index variation at the beam center $r = 0$ can be written as:

$$\Delta n_0(t) \propto n_e(r = 0, t) \propto \int_{-\infty}^t I_{pu}^{NL}(r = 0, t') dt'. \quad (1)$$

A probe beam propagating through such a gas lens undergoes a time-dependent divergence resulting in an increase of its beam size in the far field region. It has been shown in Ref. [18], that the diverging part of a field $E(t)$, isolated by the coronagraph, is proportional to $E(t)\Delta n_0(t)$. As a result, if one calls $E(t)$ the electric field of the probe to be characterized, the measured spectrogram will be of the form:

$$S(\omega, \tau) \propto \left| \int_{-\infty}^{+\infty} E(t)\Delta n_0(t - \tau) \exp(i\omega t) dt \right|^2, \quad (2)$$

where $\tau < 0$ corresponds to a probe pulse delayed relative to the pump. This expression is similar to that of a FROSt spectrogram but here the role of the switch function is played by the time-dependent refractive index variation $\Delta n_0(t)$. Typical PI-FROSt measurements, as described below, are obtained with a pump (resp. probe) of energy around 50 μ J (resp. 100 nJ) and

beam diameter $\phi = 8$ mm (resp. $\phi = 2$ mm) with a spectrometer integration time of 100 ms. The lower energy limits was found around $20 \mu\text{J}$ for the pump and 10 nJ for the probe. Further reduction in pump energy could even be achievable by selecting a gas with a lower ionization potential but one should notice that PI-FROSt arrangement already requires significantly less pump energy than that of the standard FROSt configuration.

The first trial of PI-FROSt is conducted with the characterization of NIR fs pulses centered at $\lambda = 802$ nm, i.e. for pump and probe of the same wavelength. Two typical experimental spectrograms obtained with a probe pulse that is compressed and stretched by means of a 15 mm thick SF₁₁ dispersive window are depicted in Fig. 2(a) and (c), respectively (others examples of measurements are proposed in Supplement 1). The signal

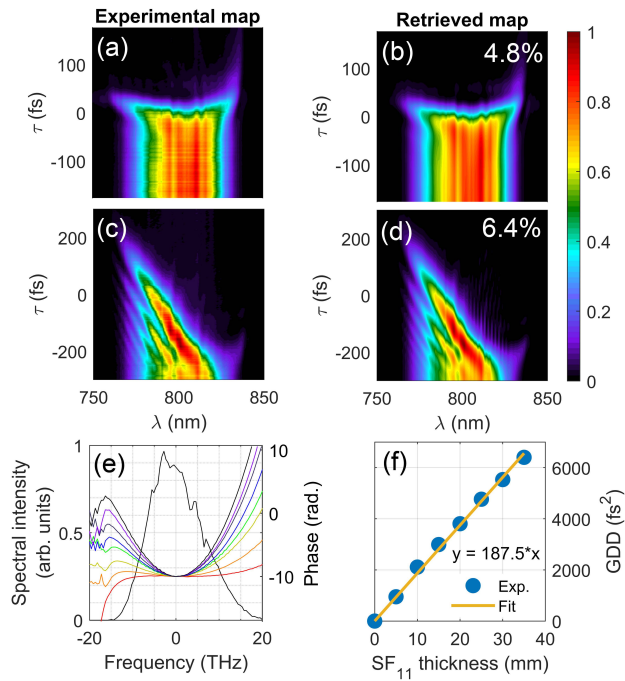


Fig. 2. PI-FROSt measurements in the NIR spectral region. (a) Experimental and (b) reconstructed spectrogram (with the reconstruction error as defined in Ref. [13]) for a compressed probe pulse. (c, d) same as (a, b) for a probe pulse after propagating through a 15 mm thick SF₁₁ dispersive plate. (e) Retrieved spectral phases and intensities for various thicknesses of SF₁₁ from 0 to 35 mm in steps of 5 mm. (f) Plot of the GDD extracted from (e) versus SF₁₁ thickness together with the corresponding fit.

obtained for a compressed probe pulse in Fig. 2(a) exhibits a notable symmetric spectral broadening for $\tau \approx 0$, i.e. for a partial overlap between the pump and probe pulses. At this delay, only the falling edge of the probe is diffracted by the switch resulting in a diffracted pulse with a duration shorter than the initial pulse (translated by a broadening in the spectral domain). Such a broadening is a clear indication that the probe pulse has undergone an ultrafast dynamic temporal cutoff. We highlight that the spectrogram showed a very high sensitivity with respect to the presence of (probe's) chirp which is manifested by the appearance of a distinct spectral asymmetry in the cutoff region. A symmetrical spectrogram, as shown in Fig. 2(a), is

achievable only through a precise adjustment of the laser compressor. The spectrogram for a probe pulse having propagated through 15 mm of SF₁₁ is depicted in Fig. 2(c). This last displays a pronounced spectral asymmetry in the cutoff region, indicating that the blue components of the spectrum have been delayed compared to the red components and are the first to diffract. It has been verified that the spectrum measured after the coronagraph for a well established plasma ($\tau \ll 0$) is perfectly identical to the input spectrum and is not modified when chirping the probe. This indicates that the spectral response of the defocusing process is constant over the bandwidth of the probe beam (which remains moderate in our conditions). The reconstructed spectrograms, displayed in Fig. 2(b) and (d), faithfully reproduce those measured. These reconstructions have been performed using a standard Levenberg Marquardt algorithm which determines the probe spectral phase to best replicate the experimental spectrogram from Eq. 2. To do this, the switch function $\Delta n_0(t)$ is directly calculated with Eq. 1 assuming a Gaussian pump pulse of 35 fs FWHM duration. However, it accounts for possible loss of temporal resolution through an effective non-linearity factor NL that is fitted by the algorithm. A procedure using a fixed NL value yields identical pulse retrieval (see Supplement 1) but the fit of NL allows slight improvement in the reconstructed spectrogram. This approach, based on a temporal switch of predefined shape with an adjusted slope, remains simpler than a blind algorithm and provides a typical error factor of between 4 and 7% (see insets of Figs. 2-3) very satisfactory, given the simplicity of the method. Several reconstructions performed in this way have been compared with the ones obtained from a ptychographic algorithm [13], which allows the retrieval of both the temporal profile of the probe and of the optical switch. The phases and the spectrogram recovered by the two methods show no discernible differences (see Supplement 1). Additional measurements were realized with other thicknesses of SF₁₁ windows, from 0 to 35 mm in steps of 5 mm. The spectral reconstruction for the set of data is depicted in Fig. 2(e). With no dispersive plate (red curve), the compressed probe pulse displays a small resulting spectral phase. The other reconstructions reveal the gradual emergence of a quadratic phase contribution above the initial phase. The retrieved phases have been fitted by a polynomial spectral function allowing to extract the Group Delay Dispersion (GDD) as a function of the SF₁₁ thickness [Fig. 2(f)]. A linear fit of these points enables to determine the value of the Group Velocity Dispersion (GVD), which yields $\phi^{(2)} = 187.5 \text{ fs}^2/\text{mm}$. This value matches very closely with the expected value of $186.7 \text{ fs}^2/\text{mm}$ at $\lambda = 802$ nm. We highlight that the measurements presented here relate to a cross-correlation where only the probe exhibits chirp. By placing the dispersive plates before the beam splitter, we have verified that the method also operates in a self-referenced configuration, provided that the pump can generate sufficient plasma to yield a reasonable signal, i.e. for moderate chirp if the energy is kept constant.

Similar measurements were carried out with a pulse in the UV spectral range by inserting the THG module in the path of the probe beam (see Fig. 1). Results are displayed in Fig. 3. In this case, it was not possible to achieve precise compression of the probe pulse, resulting in a residual positive quadratic chirp, originating from the THG module and the entrance window of the cell, as it can be seen in Fig. 3(a) and red curve of Fig. 3(e). Additional calibrated chirp have been induced by means of 6, 12, or 18 mm thick FS plates leading to a clear increase of quadratic

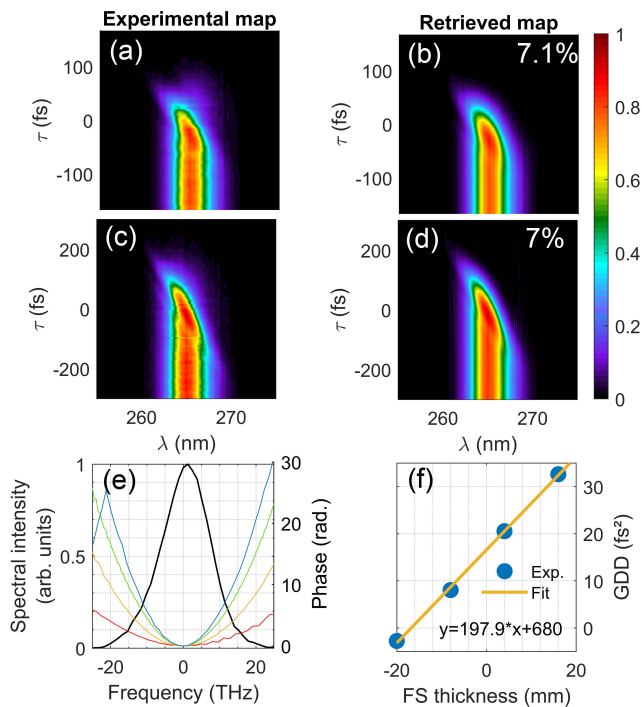


Fig. 3. PI-FROSt measurements in the UV spectral region. (a) Experimental and (b) reconstructed spectrogram of the probe pulse delivered by the THG module. (c, d) same as (a, b) for a probe pulse after propagating through a 6 mm thick FS dispersive plate. (e) Retrieved spectral phases and intensities for 0, 6, 12, and 18 mm thicknesses of FS. (f) Plot of the GDD extracted from (e) versus FS thickness together with the corresponding fit.

phase contribution in Fig. 3(e). The fit of the measured GDD as a function of the FS thickness provides a GVD $\phi^{(2)} = 197.9 \text{ fs}^2/\text{mm}$ which, once again, matches very well with the expectation of $197.5 \text{ fs}^2/\text{mm}$ at $\lambda=266 \text{ nm}$. These observations offer compelling evidence that the current approach is functional within the UV spectral range and offers a reliable and rather simple tool for the characterization of conventional ultrafast UV laser sources.

The present letter outlines the first proof-of-principle demonstration of the PI-FROSt technique. We have successfully applied the method to the characterization of conventional IR and UV fs laser pulses, achieving high-quality pulse reconstructions with a simple and robust architecture. The technique is free from phase-matching issues and potentially operates over an exceptionally broad spectral range, ultimately limited by the gas absorption in the UV range ($\approx 120 \text{ nm}$ for the first excited state of Ar) and by the plasma frequency in the far-IR range ($\approx 100 \mu\text{m}$ for an electron density of 10^{17} cm^{-3}). In addition to these advantages, PI-FROSt boasts several other strengths. It provides in-situ measurements at the beam waist with no damage threshold since the underlying mechanism relies on gas ionization. It can inherently operate with pump and probe beams of same wavelength in both self- and cross-referenced measurements. Another benefit of the method relies in the plasma recovery time. The relaxation of the PI-FROSt signal has been measured to approximately 600 ps in Ar (see Supplement 1) anticipating applicability at ultra-high repetition rates, possibly reaching GHz frequencies, while offering the possibility of measuring pulse durations up

to several tens of picoseconds. Finally, it is noteworthy that the present work was conducted in a noble gas environment to prevent any contributions from laser-induced molecular alignment [18] but recent studies (not shown here) reveal that similar results can be obtained in ambient air. Additional assessments under more challenging conditions, as for instance applications to ultra-broadband or few-cycle laser pulses, will be needed to highlight potential limitations of PI-FROSt. Investigating how the spectral response of the plasma lens and its interplay with propagation influences the outcome of the reconstruction will become crucial and may require an upgrade of the algorithm. These aspects will be explored through subsequent experimental and theoretical investigations, but this first work already highlights PI-FROSt's potential as a valuable tool for characterizing conventional femtosecond laser sources, while instilling great promise for the metrology of less conventional fields.

FUNDING

This work was supported by the Conseil Régional de Bourgogne Franche-Comté, the CNRS, the EIPHI Graduate School (contract "ANR-17-EURE-0002") and has benefited from the facilities of the SMARTLIGHT platform in Bourgogne Franche-Comté (EQUIPEX+ contract "ANR-21-ESRE-0040").

DISCLOSURES

The authors declare no conflicts of interest.

1. SUPPLEMENTAL DOCUMENT

See Supplement 1 for supporting content.

REFERENCES

- R. R. Alfano and S. L. Shapiro, Phys. Rev. Lett. **24**, 592–594 (1970).
- G. Krauss, S. Lohss, T. Hanke, A. Sell, S. Eggert, R. Huber, and A. Leitenstorfer, Nat. Photonics **4**, 33–36 (2010).
- H. Hirori, A. Doi, F. Blanchard, and K. Tanaka, Appl. Phys. Lett. **98**, 091106 (2011).
- F. Calegari, G. Sansone, S. Stagira, C. Vozzi, and M. Nisoli, J. Phys. B At. Mol. Opt. Phys. **49**, 062001 (2016).
- I. A. Walmsley and C. Dorrer, Adv. Opt. Photon **1**, 308 (2009).
- R. Trebino, K. W. DeLong, D. Fittinghoff, J. Sweetser, M. A. Krumbügel, B. Richman, and D. Kane, Rev. Sci. Instruments **68**, 3277 (1997).
- C. Iaconis and I. A. Walmsley, Opt. Lett. **23**, 792 (1998).
- M. Miranda, T. Fordell, C. Arnold, A. L'Huillier, and H. Crespo, Opt. Express **20**, 688 (2012).
- T. Oksenhendler, S. Coudreau, N. Forget, et al., Appl. Phys. B **99**, 7 (2010).
- S. B. Park, K. Kim, W. Cho, S. I. Hwang, I. Ivanov, C. H. Nam, K. T. Kim, Optica **5**, 402 (2018).
- P. Béjot, E. Szmygel, A. Dubrouil, F. Billard, B. Lavorel, O. Faucher, E. Hertz, Opt. Lett. **45**, 6795 (2020).
- D. Lee, P. Gabolde, R. Trebino, J. Opt. Soc. Am. B **25**, A34 (2008).
- A. Leblanc, P. Lassonde, S. Petit, J.-C. Delagnes, E. Haddad, G. Ernotte, M. R. Bionta, V. Gruson, B. E. Schmidt, H. Ibrahim, E. Cormier and F. Légaré, Opt. Express **27**, 28998 (2019).
- A. Leblanc, A. Longa, M. Kumar, A. Laramée, C. Dansereau, H. Ibrahim, P. Lassonde and F. Légaré, J. Phys. Photonics **3**, 045002 (2021).
- B. Brizard, A. Leblanc, S. Petit, J.-C. Delagnes, E. Cormier, H. Ibrahim, F. Légaré and P. Lassonde, Opt. Express **28**, 35807 (2020).
- K. Michelmann, U. Wagner, T. Feuer, U. Teubner, E. Förster, R. Sauerbrey, Opt. Commun. **198**, 163 (2001).
- R. Itakura, T. Kumada, M. Nakano and H. Akagi, Opt. Express **23**, 10914 (2015).
- V. Renard, O. Faucher and B. Lavorel, Opt. Lett. **30**, 70 (2005).

FULL REFERENCES

REFERENCES

1. R. R. Alfano and S. L. Shapiro, "Observation of Self-Phase Modulation and Small-Scale Filaments in Crystals and Glasses," *Phys. Rev. Lett.* **24**, 592–594 (1970).
2. G. Krauss, S. Lohss, T. Hanke, A. Sell, S. Eggert, R. Huber, and A. Leitenstorfer, "Synthesis of a single cycle of light with compact erbium-doped fibre technology," *Nat. Photonics* **4**, 33–36 (2010).
3. H. Hirori, A. Doi, F. Blanchard, and K. Tanaka, "Single-cycle terahertz pulses with amplitudes exceeding 1 MV/cm generated by optical rectification in LiNbO₃," *Appl. Phys. Lett.* **98**, 091106 (2011).
4. F. Calegari, G. Sansone, S. Stagira, C. Vozzi, and M. Nisoli, "Advances in attosecond science," *J. Phys. B At. Mol. Opt. Phys.* **49**, 062001 (2016).
5. I. A. Walmsley and C. Dorrer, "Characterization of ultrashort electromagnetic pulses," *Adv. Opt. Photon* **1**, 308 (2009).
6. R. Trebino, K. W. DeLong, D. Fittinghoff, J. Sweetser, M. A. Krumbügel, B. Richman, and D. Kane, "Measuring ultrashort laser pulses in the time-frequency domain using frequency-resolved optical gating," *Rev. Sci. Instruments* **68**, 3277 (1997).
7. C. Iaconis and I. A. Walmsley, "Spectral phase interferometry for direct electric-field reconstruction of ultrashort optical pulses," *Opt. Lett.* **23**, 792 (1998).
8. M. Miranda, T. Fordell, C. Arnold, A. L'Huillier, and H. Crespo, "Simultaneous compression and characterization of ultrashort laser pulses using chirped mirrors and glass wedges," *Opt. Express* **20**, 688 (2012).
9. T. Oksenhendler, S. Coudreau, N. Forget, et al., "Self-referenced spectral interferometry," *Appl. Phys. B* **99**, 7 (2010).
10. S. B. Park, K. Kim, W. Cho, S. I. Hwang, I. Ivanov, C. H. Nam, K. T. Kim, "Direct sampling of a light wave in air," *Optica* **5**, 402 (2018).
11. P. Béjot, E. Szmygel, A. Dubrouil, F. Billard, B. Lavorel, O. Faucher, E. Hertz, "Doppler effect as a tool for ultrashort electric field reconstruction," *Opt. Lett.* **45**, 6795 (2020).
12. D. Lee, P. Gabolde, R. Trebino, "Toward single-shot measurement of a broadband ultrafast continuum," *J. Opt. Soc. Am. B* **25**, A34 (2008).
13. A. Leblanc, P. Lassonde, S. Petit, J.-C. Delagnes, E. Haddad, G. Ernotte, M. R. Bionta, V. Gruson, B. E. Schmidt, H. Ibrahim, E. Cormier and F. Légaré, "Phase-matching-free pulse retrieval based on transient absorption in solids," *J. Opt. Soc. Am. BOpt. Express* **27**, 28998 (2019).
14. A. Leblanc, A. Longa, M. Kumar, A. Laramée, C. Dansereau, H. Ibrahim, P. Lassonde and F. Légaré, "Temporal characterization of two-octave infrared pulses by frequency resolved optical switching," *J. Phys. Photonics* **3**, 045002 (2021).
15. B. Brizard, A. Leblanc, S. Petit, J.-C. Delagnes, E. Cormier, H. Ibrahim, F. Légaré and P. Lassonde, "Single-shot phase-matching free ultrashort pulse characterization based on transient absorption in solids," *Opt. Express* **28**, 35807 (2020).
16. K. Michelmann, U. Wagner, T. Feurer, U. Teubner, E. Förster, R. Sauerbrey, "Measurement of the Page function of an ultrashort laser pulse," *Opt. Commun.* **198**, 163 (2001).
17. R. Itakura, T. Kumada, M. Nakano and H. Akagi, "Frequency-resolved optical gating for characterization of VUV pulses using ultrafast plasma mirror switching," *Opt. Express* **23**, 10914 (2015).
18. V. Renard, O. Faucher and B. Lavorel, "Measurement of laser-induced alignment of molecules by cross defocusing," *Opt. Lett.* **30**, 70 (2005).